euronoise

Numerical study of the performance of thermally isolated thermoacoustic-stacks in the linear regime

Antonio Piccolo[a] and Giuseppe Pistone[b]

[a]Dept. of Civil Engineering - Univ. of Messina, Contrada di Dio, Villaggio S.Agata, 98100 Messina, Italy
[b]Dept. of Matter Physics and Advanced Physical Technologies - Univ. of Messina, Contrada di Dio, Villaggio S.Agata, 98100 Messina, Italy
apiccolo@unime.it

A simplified calculus model to investigate on the transverse heat transport near the edges of a thermally isolated thermoacoustic stack in the low acoustic Mach number regime is presented. The proposed methodology relies on the well known results of the classical linear thermoacoustic theory which are implemented into an energy balance calculus-scheme through a finite difference technique. Details of the time-averaged temperature and heat flux density distributions along a pore cross-section of the stack are given. This information allows estimates of the optimal length of thermoacoustic heat exchangers and of the magnitude of the related heat transfer coefficients between gas and solid walls.

1 Introduction

A thermoacoustic engine consists basically of the following four components:

1. – a gas filled plane-wave resonator;
2. – an electro-acoustic transducer (acoustic driver);
3. – a porous solid medium (regenerator/stack);
4. – a couple of heat exchangers facing both ends of the stack.

In its most simple and widely studied arrangement, the stack consists of an assembly of thin parallel plates aligned in the direction x of the particle acoustic oscillation (axial or longitudinal direction) and spaced by a distance comparable to the thermal penetration depth, δ_κ, the distance through which heat can diffuse in an acoustic cycle. This element, defined as the "heart" of the engine, gives place to the desired heat/sound energy conversion, the so called "thermoacoustic effect". The heat exchangers ("hot" and "cold" exchangers), placed in close proximity of both ends of the stack, absolve to the task of either supplying or removing heat from its edges thus enabling heat transfer with the external world.

The coupling between the stack and the heat exchangers is actually recognized as a fundamental problem in thermoacoustic engines design and a major challenge for the future improvement of the overall engine's performances. Optimal design of thermoacoustic heat exchangers depends on the understanding of the thermo-fluid dynamic processes controlling the heat transfer between the sound wave and the heat exchangers at the heat exchanger−stack junctions. The starting point for the solution of this problem is the analysis of the structure of the time-averaged temperature, energy and flow fields near the pore ends of the stack.

Although considerable theoretical research has been devoted to this problem [1-3] some aspects are still not fully understood, even at low and moderate acoustic Mach numbers, such as the relative incidence of non-linear acoustic effects, turbulence, thermal effects and other local physical processes on the disagreement found between standard linear theory predictions and experiments [4].

To delve into the above phenomena, a simplified numerical model to investigate on the time-averaged temperature and energy flux distributions near the edges (both in the solid and in the gas) of a thermally isolated thermoacoustic stack is presented in this paper. The proposed methodology relies on the well known results of the classical linear thermoacoustic theory, in the "short stack" approximation formulation, for the main energy-transport variables. They are implemented into a simple energy balance calculus-scheme through a finite difference technique. The numerical results concerning the dependence of the two-dimensional temperature and energy-flux distributions on such parameters as the plate spacing, the plate thickness, the amplitude of the resonant wave, etc., are presented. Information on the optimal length of thermoacoustic heat exchangers and on the magnitude of the related convective heat transfer coefficient between working gas and solid wall is also derived.

2 Formulation

For problems characterized by a periodic time dependence (like thermoacoustics), the time-averaged law of conservation of energy for a compressible viscous fluid is expressed by the equation [5]:

$$\nabla \cdot \dot{\mathbf{e}} = 0 \tag{1}$$

Integrating this equation over a volume element bounded by a closed surface S and applying the divergence theorem gives us:

$$\oint_S \dot{\mathbf{e}} \cdot \mathbf{n}\, dS = 0 \tag{2}$$

where $\mathbf{n}$ is the unit vector directed along the normal to the surface element dS. Equation (2) can be conveniently applied to whatever sub-region traced in the gas to impose local energy balance. To accomplish this, a finite difference technique may be used, where the quantitative results of standard linear theory can be considered for the components of the time-averaged energy flux density along the directions of interest.

The thermoacoustic equation for the hydrodynamic energy flux density along the x direction is derived in the simplified case of a parallel-plate stack. The ratio of the plate spacing (and of the plate thickness) to the width in the transverse direction is taken to be very small (as in real cases) thus the energy flow along the z direction (perpendicular to the x-y plane) is negligible and the problem can be regarded as two-dimensional.

The conventional complex notation is adopted for the time-dependent variables:

$$\xi(t) = \xi_m + \mathrm{Re}\left\{\xi_1 e^{i\omega t}\right\} \tag{3}$$

where t is the time, i the imaginary unit, Re{ } signifies the real part and where the mean value ξ_m is real but the amplitude oscillation ξ_1 is complex to account for both magnitude and phase of the oscillation at frequency ω.

If the equation of state of the gas is taken to be the ideal gas equation, the following expression holds for the time-averaged hydrodynamic enthalpy flow along the longitudinal direction [6]:

$$\dot{h}_x = \rho_m c_P \frac{\omega}{2\pi} \int_0^{2\pi/\omega} T(t)\, u(t)\, dt = \frac{1}{2} \rho_m c_P \,\mathrm{Re}\{T_1 \tilde{u}_1\} \qquad (4)$$

where ρ_m is the mean density of the gas, c_P is the isobaric specific heat of the gas, T is the temperature, u is the x-component of the acoustic particle velocity, and tilde indicates complex conjugation. To evaluate this quantity, explicit expressions for the first-order complex amplitudes T_1 and u_1 inside the stack are required. If the specific heat of the plate material, c_s, is notably greater than c_P, the following expressions hold for T_1 and u_1 [6]:

$$T_1 = \frac{1}{\rho_m c_P}(1-h_\kappa)P_1 - \frac{1}{\rho_m \omega^2}\frac{dP_1}{dx}\frac{dT_m}{dx}\left[\frac{(1-h_\kappa)-\mathrm{Pr}\,(1-h_\nu)}{(1-\mathrm{Pr})}\right] \qquad (5)$$

$$u_1 = \frac{i}{\omega\rho_m}\frac{dP_1}{dx}(1-h_\nu) \qquad (6)$$

where

$$h_\kappa = \frac{\cosh[(1+i)y/\delta_\kappa]}{\cosh[(1+i)y_0/\delta_\kappa]} \qquad h_\nu = \frac{\cosh[(1+i)y/\delta_\nu]}{\cosh[(1+i)y_0/\delta_\nu]} \qquad (7)$$

P_1 being the local amplitude of the dynamic pressure, Pr the Prandtl number, y_0 half distance between two plates, δ_ν the viscous penetration depth and where y=0 is in the center of the fluid gap.

Run	y_0/δ_κ	l/δ_κ	ξ_s/λ	P_A/P_m
1	3.39	0.088	0.131	0.017
2	2.1	1.3	0.179	0.02
3	0.5 - 4	1.271	0.179	0.02
4	0.25 - 0.75	0.339	0.179	0.025
5	1 - 1.25	0.53	0.179	0.025
6	1.5 - 2	0.805	0.179	0.025
7	2.5 - 3	1.271	0.179	0.025
8	1	0.551	0.179	0.06
9	1.5	0.805	0.179	0.06
10	2	1.059	0.179	0.06
11	2.5	1.271	0.179	0.06
12	3	1.568	0.179	0.06

Table 1. Parameters of selected simulations. Test gas = helium, mean temperature = 300 K, mean pressure = 10 kPa, resonator length = $\lambda/2$=5.04 m, resonance frequency = 100 Hz, plate material thermal conductivity = 10 $\mathrm{Wm^{-1}K^{-1}}$; L_S/λ = 0.025.

A simple expression for the pressure derivative dP_1/dx can be derived if the stack satisfies the "short stack approximation". Under this condition pressure and velocity may be approximated at the entrance of the stack in terms of the equations given by loseless acoustics that, in the case of a half-wavelength resonator, are simply:

$$P_1 = P_A \sin k x_s = P_0 \qquad (8)$$

$$u_1 = i\frac{P_A}{\rho_m a}\cos k x_s = i u_0 \qquad (9)$$

P_A being the amplitude of the dynamic pressure at a pressure antinode, k the wave number (k=2π/λ), a the sound velocity and x_s the mean stack location calculated as the distance of the stack from the centre of the resonator.

Using equation (9), we can write for the volume flow rate at the entrance of the stack

$$U_1 = A_{res} u_1 = i\, A_{res} u_0 \qquad (10)$$

A_{res} being the cross sectional area of the resonator. Equation (6) can be integrated over the cross section of a pore to obtain U_1 within the stack

$$U_1 = \frac{A_s}{y_0}\int_0^{y_0} u_1(y)\,dy = \frac{i\,A_s}{\omega\rho_m}\frac{dP_1}{dx}(1-f_\nu) \qquad (11)$$

where

$$f_\nu = \frac{\tanh[(1+i)y_0/\delta_\nu]}{[(1+i)y_0/\delta_\nu]} \qquad (12)$$

and where A_s is the cross sectional area of the stack open to gas flow. By imposing now continuity of volume flow rate at the entrance of the stack, equations (10) and (11) can be equated to find dP_1/dx just inside and, by approximation, along the stack

$$\frac{dP_1}{dx} = \frac{u_0}{\Omega}\frac{\rho_m \omega}{(1-f_\nu)} \qquad (13)$$

where the blockage ratio $\Omega = A_s/A_{res} = 1/(1+l/y_0)$ describes the porosity of the stack.

Substituting now equations (8) and (13) into equations (5) and (6) and these last in equation (4), the following expression is found, at second order in the acoustic oscillation amplitude, for $\dot{h}_x$:

$$\dot{h}_x = \frac{1}{2\Omega}\mathrm{Im}\left[\frac{(1-\tilde{h}_\nu)(1-h_\kappa)}{(1-\tilde{f}_\nu)}\right]P_0\,u_0 - \frac{c_P\rho_m}{2\omega\Omega^2(1-\mathrm{Pr})}\frac{dT_m}{dx}\mathrm{Im}\left[\frac{(1-h_\kappa)(1-\tilde{h}_\nu)}{|1-f_\nu|^2}\right]u_0^2 \qquad (14)$$

Note that for a given stack location (x_s) in the resonator, all quantities in this equation may be assumed independent of the axial coordinate x within the stack except T_m; quantities enclosed in square brackets, on the other hand, depend only on the y coordinate reflecting the transverse variations of

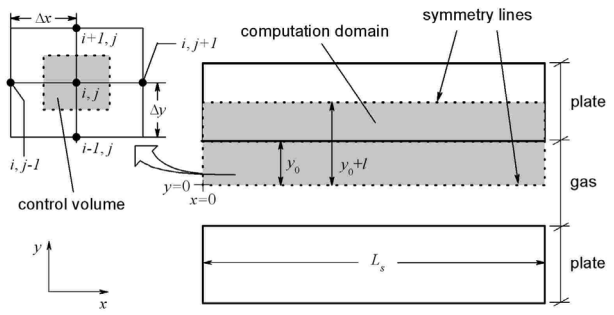

Fig. 1. Magnified region of two stack plates. The light grey areas indicate the computation domain and the control volume about a generic nodal point.

the acoustic velocity u_1 and of the oscillatory temperature T_1. In the following we rewrite equation (14) in the form

$$\dot{h}_x(x,y) = \dot{h}_\alpha(y) - \frac{\partial T_m(x,y)}{\partial x}\dot{h}_\beta(y) \tag{15}$$

where

$$\dot{h}_\alpha(y) = \frac{1}{2\Omega}\mathrm{Im}\left[\frac{(1-\tilde{h}_\nu)(1-h_\kappa)}{(1-\tilde{f}_\nu)}\right]P_0 u_0 \tag{16}$$

and

$$\dot{h}_\beta(y) = \frac{c_P \rho_m}{2\omega\Omega^2(1-\mathrm{Pr})}\mathrm{Im}\left[\frac{(1-h_\kappa)(1-\tilde{h}_\nu)}{|1-f_\nu|^2}\right]u_0^2 \tag{17}$$

are both real and positive quantities.

The energy flux density along the axial direction comprises also the diffusive term $-K\partial T_m/\partial x$ (K being the thermal conductivity of the gas). This contribution is generally considered to be negligible in comparison to the hydrodynamic-one and will be here neglected.

On the opposite hand, the transverse component of the energy flux density contains, by hypothesis, only the diffusive term

$$\dot{q}_y = -K\frac{\partial T_m}{\partial y} \tag{18}$$

where $\dot{q}_y$ is the time-averaged heat flux density along the transverse direction.

Since a x-dependent derivative $\partial T_m/\partial x$, and thus a x-variable $\dot{h}_x$ along the stack, implies net heat deposition into and/or extraction out of the solid plates, equations (15) and (18) must be related to the analogues in the solid walls. If K_s is the thermal conductivity of the plate material, the time-averaged heat flux densities along the x and y directions are simply

$$\dot{q}_x = -K_s\frac{\partial T_{sm}}{\partial x} \qquad \dot{q}_y = -K_s\frac{\partial T_{sm}}{\partial y} \tag{19}$$

after taking into account that thermal conduction is the unique mechanism of energy transport inside the stack plates and that, being by hypothesis $c_s >> c_p$, the solid temperature oscillations are negligible.

3 Numerical model

The simulation model system is a thermally isolated stack of parallel plates, of length L_s located at position x_s in a half-wavelength gas filled resonator sustaining a standing acoustic wave. As a stack is usually constituted by a set of identical plates, calculations were performed in a single channel of the stack, i.e. between a single pair of parallel plates. The simulation domain is further reduced by symmetry from half a gas duct to half a plate and is indicated in Figure 1 by the light grey area together with the coordinate system used. The axis parallel to the plates is the x axis; x=0 is chosen to be the beginning of the stack on the left. The y axis is perpendicular to the stack-plates; y=0 is chosen to be the midpoint between the two adjacent plates.

The calculation of the steady-state two-dimensional time-averaged temperature distribution was performed using a finite difference methodology. To this end, the computational domain was subdivided using a rectangular grid. In the x direction the computation mesh size, Δx, was typically $0.0041L_s$ while in the y direction the computation mesh size, Δy, was typically $0.02y_0$. The set of finite-difference equations for the unknown quantities $T_m(x, y)$ and $T_{sm}(x, y)$ was then derived imposing energy balance at each nodal point of the computational grid making use of

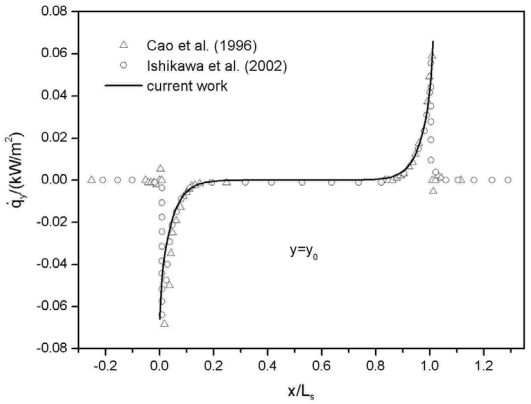

Fig. 2. Time-averaged heat flux density in the y direction at the plate surface (y=y_0) as a function of the position along the plate. Solid line is the heat flux density profile computed using the present model (run 1). Open triangles are numerical data from ref. 1 (run 2). Open circles are numerical data from ref. 3 (run 7).

equations (15) and (18) for the x and y components of the energy flux density in the gas and of equations (19) for the analogues in the solid. Temperature spatial gradients were discretized using first order nodal temperature differences. As an example, for a nodal point laying in the gas region of the simulation domain (see Figure 1) the resulting equation is:

$$K\frac{\Delta x}{\Delta y}T_m^{i-1,j} + \dot{h}_\beta\frac{\Delta y}{\Delta x}T_m^{i,j-1} + \left(-2\dot{h}_\beta\frac{\Delta y}{\Delta x} - 2K\frac{\Delta x}{\Delta y}\right)T_m^{i,j} + \dot{h}_\beta\frac{\Delta y}{\Delta x}T_m^{i,j+1} + K\frac{\Delta x}{\Delta y}T_m^{i+1,j} = 0 \tag{20}$$

which is equation (2) applied to the control volume about node (i, j). Analogue equations yield for nodal points laying in the plate, while to derive the system-equations for nodal points laying on boundary lines, symmetry lines and on the gas-plate interface line, the following boundary conditions were imposed:

- nodal lines at y=0 and y=y_0+l are symmetry lines so

$$\left(\frac{\partial T_m}{\partial y}\right)_{y=0} = 0 \qquad \left(\frac{\partial T_{sm}}{\partial y}\right)_{y=y_0+l} = 0 \tag{21}$$

- continuity conditions at the fluid-solid interface (y=y_0) entail that the time-averaged temperature of the gas corresponds to the plate temperature and that the energy flux leaving (or entering) the gas equals that entering (or leaving) the solid wall

$$T_m(y=y_0) = T_{sm}(y=y_0);\ K\left(\frac{\partial T_m}{\partial y}\right)_{y=y_0} = K_S\left(\frac{\partial T_{sm}}{\partial y}\right)_{y=y_0} \tag{22}$$

• for a thermally isolated stack no heat may leave or enter the stack diffusively across the plates terminations ($y_0 \leq y \leq y_0+l$)

$$\left(\frac{\partial T_{sm}}{\partial x}\right)_{x=0} = 0 \qquad \left(\frac{\partial T_{sm}}{\partial x}\right)_{x=L_s} = 0 \qquad (23)$$

• for a thermally isolated stack no energy may leave or enter the stack hydrodynamically across the pore ends ($0 \leq y < y_0$)

$$\dot{h}_x(x=0) = 0 \qquad \dot{h}_x(x=L_s) = 0 \qquad (24)$$

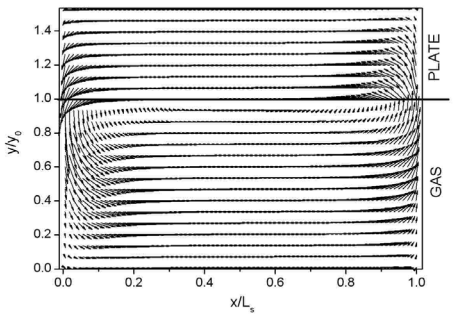

Fig. 3. Time-averaged energy vector pattern for $y_0/\delta_\kappa = 2.1$ and $l/\delta_\kappa = 1.3$ (run 2) in the whole computation domain.

The elements of the coefficient matrix associated to the resultant system of linear algebraic equations were calculated using a code developed by the authors in FORTRAN-77 language and the system was solved using a LU decomposition with partial pivoting and row interchanges matrix factorization routine. The latter was taken from the LAPACK library routines available online at [7]. Details about accuracy, computation cost, etc. can be found in [7]. Once the time-averaged temperature distribution is known, it can be substituted in equations (15), (18) and (19) to determine the energy flux distributions along the x and y directions both in the gas and in the plate.

4 Results and discussion

Numerical simulations are carried out varying P_A, y_0 and l. The parameters of different runs are listed in Table 1.Helium at a mean temperature of 300 K and at a mean pressure of 10000 Pa is assumed as working fluid. It is considered enclosed in a half-wavelength resonator 5.04 m length having a fundamental resonance frequency of 100 Hz. These operating conditions are chosen to facilitate the comparison with the test cases of Cao et al. [1] and of Ishikawa et al. [3].

The test of the proposed model predictions against the results from previous numerical studies is illustrated Figure 2 where the transverse component of the heat flux density at the gas-solid interface ($y = y_0$) for run 1 is compared with run 2 of Cao et al. [1] and run 7 of Ishikawa et al. [3]. A quite perfect overlapping is found in spite of the fact that in these models different simulation domains and boundary conditions are specified. The simulation reproduces the result that the transverse heat flux is sharply peaked near the plate extremities being zero elsewhere. This is a clear evidence of the fact that a net heat exchange between fluid and solid takes place only at the plate edges. In particular, $|\dot{q}_y|$ exhibits a monotonic increase reaching a maximum when the end sections are approached: $\dot{q}_{y,max} = |\dot{q}_y(x=0, y=y_0)| = |\dot{q}_y(x=L_s, y=y_0)|$.

Since the time-averaged energy flux at the plate surface is positive when entering the plate and negative when leaving the plate, Figure 2 implies that over the period of an acoustic cycle, energy flows out of the left end of the plate, down along the thermal boundary layer in the gas and into the right end of the plate. In the hypothesis of a thermally insulated stack, these energy flows are supplied by the plates themselves, which thus cool at the end which supplies the energy, and heat at the other end which absorbs it. The right hand edge therefore behaves as a heat sink while the left hand edge acts as a heat source. In steady-state the resulting temperature gradient developed in the plate is inversely proportional to its thermal conductivity and of such magnitude that the hydrodynamic energy flow in the gas is perfectly balanced by a return diffusive heat flow in the wall. The overall energy transfer process is clearly displayed for run 2 in Figure 3 where the time-averaged energy vectors describe a closed "loop".

To get insight into the optimum length of the heat exchanger fins it is necessary to analyze the distance from the plate end over which a significant non-zero time-averaged heat transfer between solid and gas takes place.

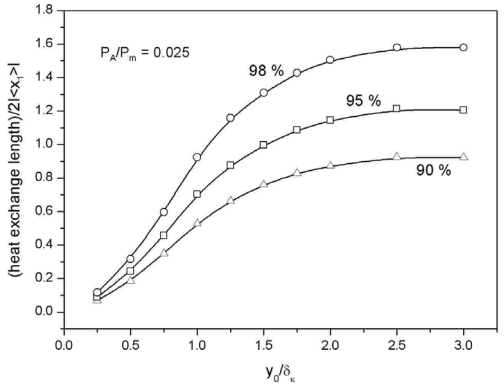

t

Fig. 4. Heat exchange length (distance from the plate edge over which the net heat transfer between gas and solid amount to 90%, 95% and 98% of the heat totally transferred) nomalized by $2|\langle x_1 \rangle|$ v.s. plate spacing for $P_A/P_m = 0.025$ (runs 4-7).

The dependence of the heat exchange length on the plate spacing is analyzed in Figure 4 where the distance from the plate edge over which the net heat transferred between gas and solid amounts to 90% 95% and 98% of the total heat transferred (inferred from the transverse component of the heat flux density at the solid boundary $\dot{q}_y$) is reported as a function of the plate spacing for $P_A/P_m = 0.025$ (P_m being the mean pressure of the gas). In the graph three regions are clearly distinguishable:

I – for $y_0/\delta_\kappa < 1$the length available for heat transfer increases very fast at increasing the plate spacing, still remaining lower than $2|\langle x_1 \rangle|$;

II – for $1 < y_0/\delta_\kappa < 2$ the curves exhibit a less marked growth. In this range for a heat exchange length equal to $2|<x_1>|$ the net thermal power exchanged between gas and solid varies from 92 to 99 % of the total power transferred;

III – for $y_0/\delta_\kappa > 2$ the curves become flat denoting how the heat exchange length no more depends upon the plate spacing. In this range for a heat exchange length equal to $2|<x_1>|$ the net thermal power exchanged between gas and solid amounts to 92% of the power totally transferred.

From the above considerations it follows that, as the plate spacing of real devices are generally found in range II, the peak-to-peak particle displacement amplitude can be conveniently assumed as useful length for the heat exchangers fins, as generally conjectured on heuristic grounds. The reduced heat exchange length found for very short plate spacing ($y_0/\delta_\kappa < 1$) is in agreement with the findings of Cao et al. [1] who ascribed this behavior to the improved thermal contact attending tightly spaced fins which reduces the phase lag between pressure and motion below the optimal value for which $\dot{h}_x$ peaks.

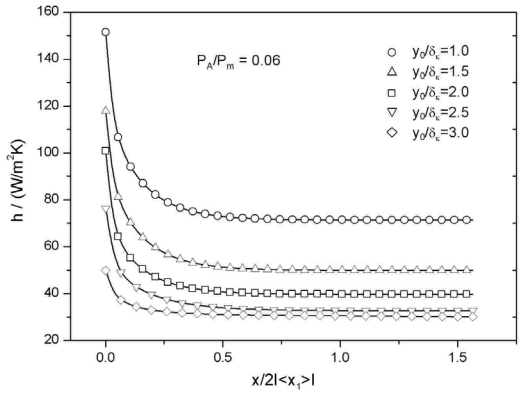

Fig. 5. Convective heat transfer coefficient between gas and solid v.s. $x/2|<x_1>|$ at selected plate spacing for P_A/P_m = 0.06 (runs 8-12).

Numerical simulations performed at different plate thickness l (not shown) reveal that this parameter has little influence on the gas-solid heat exchange area: for a thermally isolated stack the plate simply serves as a duct which "closes" the energy flux path.

For estimation of the heat transfer coefficient between gas and solid walls of thermoacoustic heat exchangers reference is made to the well known definition-law of h as reported in standard textbooks [8]:

$$h = \frac{K\left|\frac{\partial T_m}{\partial y}\right|_{y=y_0}}{\left|T_{sm}(y_0) - T_m\right|} \qquad (25)$$

which combines the Newton's law of cooling with the boundary condition that at the solid surface, being no fluid motion, energy transfer occurs only by conduction. This relation allows for estimation of the local convective heat transfer coefficient once the transverse temperature gradient is known, so it can be conveniently applied in the proposed numerical calculus. Since in relation (18) T_m represents the temperature of the bulk fluid in all performed simulations a plate spacing $y_0 \geq \delta_\kappa$ is chosen and T_m is evaluated at the centre of the pore: $T_m = T_m(y = 0)$.

In Figure 5 the dependence of h on the normalized longitudinal coordinate $x/2|<x_1>|$ at selected plate spacing is shown. The local convective coefficient varies with x attaining, at a distance greater than $2|<x_1>|$, a constant value which depends, in turn, on the plate spacing; this dependence disappears for $y_0/\delta_\kappa > 2.5$, the curves almost overlapping each other.

5 Conclusions

In this paper a numerical calculus scheme has been developed by implementing the simplified linear thermoacoustic theory – the short stack approximation – into a simple energy conservation model through a finite difference methodology. The essential features of the time-averaged temperature and heat flux density distributions near the edges of a thermally isolated thermoacoustic stack are investigated. The simulation results agree well with those of other numerical computations available in literature. The model allows to enquire on the optimal length of thermoacoustic heat exchangers and on the magnitude of the related heat transfer coefficients between gas and solid walls.

In its current form, the model is expected to be valid when restricted to situations where the classical solution for the amplitude of the temperature oscillations T_1 may be retained accurate near the pore terminations. This should be reasonably verified when transverse temperature gradients are weak, namely when stacks are operated at low Mach number (typically less than a few percent).

References

[1] Cao N., Olson J.-R., Swift G.-W., Chen S., Energy flux density in a thermoacoustic couple, J. Acoust. Soc. Amer. 99 (1996) 3456-3464.

[2] Worlikar A.-S., Knio O.-M., Numerical simulation of a thermoacoustic refrigerator I. Unsteady Adiabatic flow around the stack, J. Comput. Phys. 127 (1996) 424-451.

[3] Ishikawa H., Mee D.-J., Numerical investigations of flow and energy fields near a thermoacoustic couple, J. Acoust. Soc. Amer. 111 (2002) 831-839.

[4] Atchley A.-A, Hofler T.-J., Muzzerall M.-L., Kite M.-D., Ao C., Acoustically generated temperature gradients in short plates, J. Acoust. Soc. Amer. 88 (1990) 251-263

[5] Landau L.D., Lifshitz E.M., Fluid Mechanics, first ed., Pergamon, London, 1959, pp. 184.

[6] Swift G.-W., Thermoacoustic engines, J. Acoust. Soc. Amer. 84 (1988) 1145-1180.

[7] http://www.netlib.org/lapack

[8] F. Incoprera, D. Dewitt, Fundamentals of Heat and Mass Transfer, third ed., Wiley and Sons, New York, 1996, pp. 130, 320, 395, 495.